DOI: 10.1002/anie.201408623

Mesostructured Zeolites

Co-development of Crystalline and Mesoscopic Order in Mesostructured Zeolite Nanosheets**

*Robert J. Messinger, Kyungsu Na, Yongbeom Seo, Ryong Ryoo, and Bradley F. Chmelka**

Abstract: *Mesoporous zeolites are a new and technologically important class of materials that exhibit improved diffusion and catalytic reaction properties compared to conventional zeolites with sub-nanometer pore dimensions. During their syntheses, the transient developments of crystalline and mesoscopic order are closely coupled and challenging to control. Correlated solid-state NMR, X-ray, and electron microscopy analyses yield new molecular-level insights on the interactions and distributions of complicated organic structure-directing agents with respect to crystallizing zeolite frameworks. The analyses reveal the formation of an intermediate layered silicate phase, which subsequently transforms into zeolite nanosheets with uniform nano- and mesoscale porosities. Such materials result from coupled surfactant self-assembly and inorganic crystallization processes, the interplay between which governs the onset and development of framework structural order on different length and time scales.*

Surfactant-directed zeolites with mesostructural order often exhibit improved transport, adsorption, and reaction properties compared to conventional zeolites, especially with respect to large molecules.[1–5] During their syntheses, coupled framework crystallization and surfactant self-assembly processes occur that are not well understood and are challenging to control. Here, we elucidate the molecular-level processes and interactions that underpin simultaneous inorganic crystallization and surfactant-directed ordering during the syntheses of mesostructured zeolite silicalite-1, the siliceous analog of the technologically important aluminosilicate zeolite ZSM-5 catalyst with an MFI-type structure. Transient local compositions, atomic and mesoscale structures, and surfactant-framework interactions are monitored by ex situ solid-state nuclear magnetic resonance (NMR) spectroscopy, X-ray diffraction (XRD), and high-resolution transmission and scanning electron microscopy (TEM, SEM) measurements. The analyses establish the development and evolution of transient framework structures during hydrothermal synthesis, revealing that siliceous zeolite MFI nanosheets form through intermediate nanolayered frameworks with 2D crystal-like structures.

Generally, mesoporous zeolites can be synthesized by balancing colloidal aggregation, surfactant self-assembly, and zeolite crystallization processes. Synthesis strategies have relied on controlling aggregation of pre-nucleated zeolite nanocrystals, such as by grafting hydrophobic species to the nanoparticle surfaces,[6] or by directing their self-assembly into mesostructured frameworks with organosilane species.[7,8] Alternatively, zeolites with mesostructural order can be synthesized by co-assembly of novel structure-directing surfactants with inorganic precursors that subsequently condense and crystallize, while maintaining high extents of uniform mesoscale order.[1,2]

Until now, little has been known about how such self-assembled and crystalline frameworks develop and how their structures transform over different length and time scales. The majority of surfactant-directed materials with mesostructural order previously reported exhibit amorphous frameworks, such as MCM-[9] or SBA-type[10] mesoporous silicas. Early attempts at synthesizing such materials with crystalline frameworks used combinations of structure-directing species that tended to form separate zeolitic or mesostructured materials, producing either bulk zeolites, amorphous mesoporous materials, or their physically segregated mixtures.[11,12] Surfactant-directed materials with both long-range atomic and mesoscopic order were synthesized using mono-quaternary ammonium surfactants that led to nanolayered silicates with 2D crystal-like frameworks, although they were fragile and non-porous.[13] By comparison, multi-quaternary ammonium surfactants have been shown to lead to more structurally robust mesostructurally ordered zeolites with both highly uniform bimodal nano- and mesoscale porosities and technologically important catalytic reaction properties.[1,2] Few such materials have been synthesized, in part because of the difficulty of characterizing and controlling the coupled crystallization and self-assembly processes.

For the case of mesostructured zeolite MFI nanosheets, the development and evolution of crystalline and mesostruc-

[*] Dr. R. J. Messinger, Prof. Dr. B. F. Chmelka
Department of Chemical Engineering
University of California
Santa Barbara, CA 93106 (USA)
E-mail: bradc@engineering.ucsb.edu
Dr. K. Na, Dr. Y. Seo, Prof. Dr. R. Ryoo
Department of Chemistry
Korea Advanced Institute of Science and Technology
Daejeon 305-701 (Republic of Korea)
Dr. Y. Seo, Prof. Dr. R. Ryoo
Center for Nanomaterials and Chemical Reactions
Institute for Basic Science
Daejeon 305-701 (Republic of Korea)

[**] We thank Dr. S. Cadars for helpful discussions. This work was supported by the US NSF under grant number CHE-0924654 and the US DOE through the IMMS at Los Alamos National Laboratory. R.J.M. is grateful to the Warren and Katharine Schlinger Foundation for a doctoral fellowship. NMR measurements were conducted using the Central Facilities of the UCSB Materials Research Laboratory, which are supported by the NSF MRSEC Program under award number DMR-1121053. K.N., Y.S., and R.R. acknowledge support from the IBS under grant number CA1401.

Supporting information for this article is available on the WWW under http://dx.doi.org/10.1002/anie.201408623.

tural order are highly coupled. Initially, products form with weak mesophase ordering and amorphous frameworks that transform into about 1 nm-thick silicate sheets with high extents of 2D atomic order, which subsequently crystallize into assemblies of mesostructured zeolite MFI nanosheets with 3D atomic order (Figure 1). For example, after 1 day, the

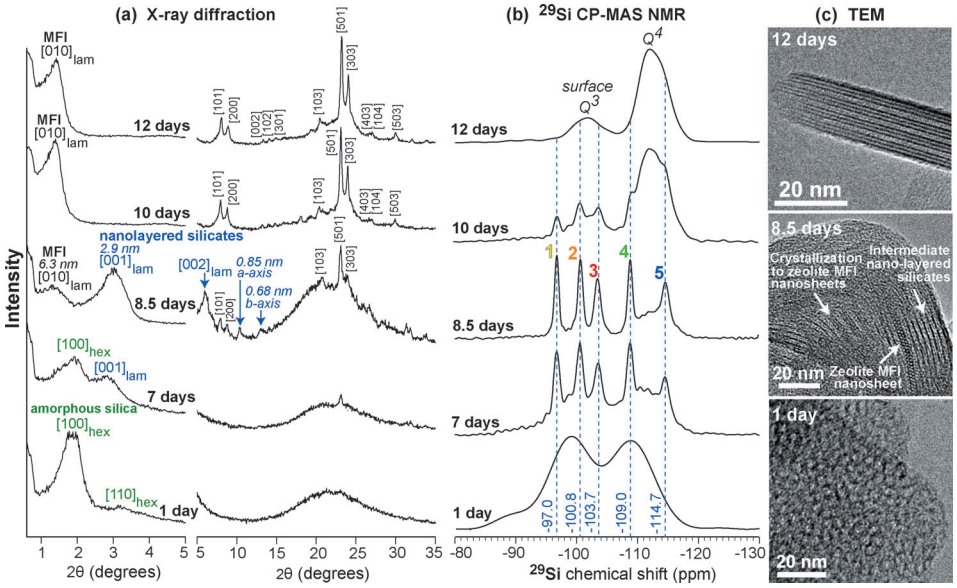

Figure 1. a) Small- and wide-angle powder XRD patterns, b) solid-state ^{29}Si CP-MAS NMR spectra, and c) representative TEM images[14] of the products obtained after 1, 7, 8.5, 10, and 12 days during hydrothermal synthesis (130 °C) of mesostructured zeolite MFI nanosheets. XRD reflections are labeled with respect to the different characteristic material structures: initially amorphous silica frameworks with weak hexagonal mesophase ordering (green), intermediate nanolayered silicates (blue), and zeolite MFI nanosheets (black).

small- and wide-angle XRD patterns (Figure 1 a) of the intermediate product exhibit reflections that are consistent with a weakly ordered hexagonal mesophase (unit cell parameter 5.4 nm), as corroborated by TEM (Figure 1 c), and an atomically disordered silica framework. The ^{29}Si cross-polarization magic-angle spinning (CP-MAS) spectrum (Figure 1 b) shows three broad, overlapping signals at −89, −98, and −109 ppm, corresponding to amorphous Q^2, Q^3, and Q^4 ^{29}Si moieties, respectively, with increasing extents of cross-linking. After 7 and 8.5 days, the small-angle XRD reflections indicate the appearance of a developing lamellar mesostructure (d-spacing 2.9 nm), as corroborated by TEM, while the ^{29}Si CP-MAS spectra reveal five resolved ^{29}Si signals at −97.0, −100.8, −103.7, −109.0, and −114.7 ppm (labeled 1–5) that reflect the development of appreciable short-range atomic order. Interestingly, these isotropic ^{29}Si chemical shifts are identical to those reported for a nanolayered silicate[13,15–16] synthesized under similar conditions, but using a mono-quaternary ammonium surfactant. The wide-angle XRD pattern also exhibits reflections that are consistent with the a and b axes of these nanolayered silicates (d-spacings of 0.85 and 0.68 nm, respectively),[13,15–16] comparisons of which are shown in the Supporting Information (Figure S1).

After 10 and 12 days of hydrothermal synthesis, the XRD patterns (Figure 1 a) show scattering intensities that are indexable to zeolite MFI frameworks with lamellar mesophase ordering (d-spacing 6.3 nm), as corroborated by TEM (Figure 1 c). The ^{29}Si CP-MAS spectra (Figure 1 b) reveal that the five ^{29}Si signals from the nanolayered silicate intermediate exhibit diminished intensity and eventually disappear, as MFI crystallization is completed after 12 days.[1] They are replaced by broad ^{29}Si signals centered at −101 and −112 ppm, associated with surface Q^3 and Q^4 ^{29}Si moieties of the MFI frameworks, which contain at least 24 crystallographically distinct ^{29}Si sites, though the signals of which are overlapping in the 1D spectrum.[18] The zeolite MFI nanosheets thus appear to form through an atomically ordered nanolayered intermediate, as governed by the coupled influences of zeolite- and mesostructure-directing moieties of the surfactant species. Interestingly, the XRD, NMR, and TEM measurements all show evidence (Figure 1) that the zeolite MFI nanosheets have begun to crystallize after seven days of hydrothermal synthesis.

Importantly, the di-quaternary ammonium headgroups of the surfactant species direct the formation of both the intermediate silicate and zeolite MFI frameworks, as established by the solid-state 2D ^{29}Si{^{1}H} HETCOR NMR spectrum (Figure 2) acquired on the intermediate product after 8.5 days of hydrothermal synthesis. Strong 2D intensity correlations are observed between the five ^{29}Si signals from the nanolayered silicate framework (blue dashed lines) and the ^{1}H signal at 3.3 ppm from the quaternary ammonium moieties $N^+C\mathbf{H}_2$- (d) and $N^+C\mathbf{H}_3$ (e) of the surfactant headgroups, establishing their mutual interactions. This same ^{1}H signal is also correlated with partially resolved ^{29}Si signals from −111 to −113 ppm associated with developing and crystallized Q^4 sites in the MFI framework (red dashed lines). 2D intensity correlations are also observed between the same ^{29}Si signals from the nanolayered silicate and MFI frameworks and the ^{1}H signal at 1.5 ppm from the surfactant C_6 alkyl chains (b,c). After 12 days, an analogous 2D ^{29}Si{^{1}H} HETCOR spectrum (Figure S2) acquired on the mesostructured zeolite MFI product reveals similar correlated intensity between ^{29}Si signals from incompletely condensed (likely surface) Q^3 and Q^4 MFI sites and ^{1}H signals associated with both $N^+C\mathbf{H}_2$- and $N^+C\mathbf{H}_3$ headgroup moieties (d,e) and the C_6 alkyl chains (b,c). The 2D ^{29}Si{^{1}H} HETCOR spectra thus establish strong interac-

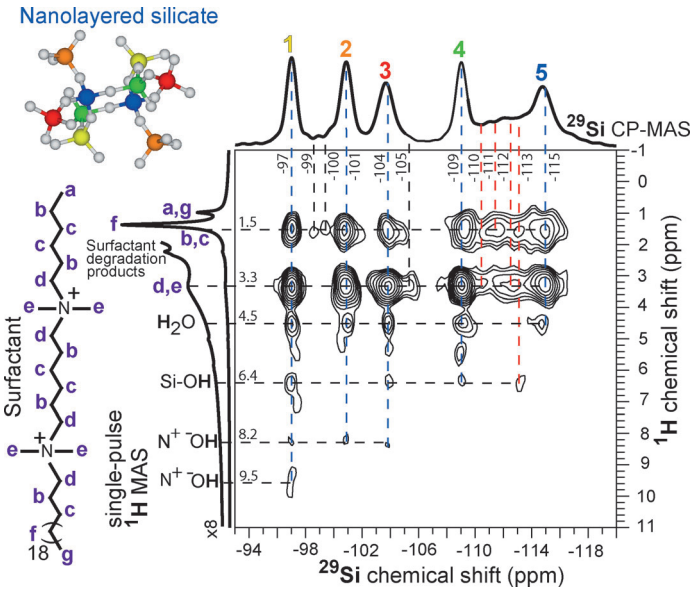

Figure 2. Solid-state 2D $^{29}Si\{^{1}H\}$ HETCOR NMR spectrum of the intermediate product of crystallizing zeolite MFI nanosheets after 8.5 days of hydrothermal synthesis. 1D ^{29}Si CP-MAS and single-pulse ^{1}H MAS NMR spectra are shown along the horizontal and vertical axes, respectively. A schematic diagram of a di-quaternary-ammonium surfactant molecule is labeled with ^{1}H signal assignments (a–g) of covalently bonded hydrogen atoms.

tions between the surfactant headgroups and linking C_6 alkyl segments with both the nanolayered silicate and zeolite MFI frameworks.

Electron microscopy measurements performed on materials at intermediate stages of zeolite crystallization provide additional insights into how the nanolayered intermediate silicates transform into the zeolite MFI nanosheets. The TEM image acquired on the product after 8.5 days of hydrothermal synthesis (Figure 1c) shows regions where the nanolayered silicates are crystallizing into zeolitic structures within the same domains. SEM images of the same material (Figure 3) reveal characteristic morphologies associated with the nanolayered silicates, zeolitic MFI nanosheets, and crystallizing regions, which co-exist within the same particle. These results corroborate the molecular insights provided by 2D NMR spectroscopy (Figure 4a), which establish that zeolite crystallization under these conditions occurs within the same domains and not by dissolution and re-precipitation.

Direct evidence for the conversion of the nanolayered silicate intermediates into the zeolite MFI nanosheets is established by 2D $^{29}Si\{^{29}Si\}$ correlation NMR spectra, which reveal interactions between pairs of dipole–dipole-coupled ^{29}Si framework sites, as they are in the process of transforming. The 2D $^{29}Si\{^{29}Si\}$ NMR spectrum acquired for the intermediate product (99% ^{29}Si-enriched) after 10 days of hydrothermal synthesis (Figure 4a) exhibits numerous resolved ^{29}Si signals that are correlated across the diagonal (black dotted line), manifesting the mutual proximities (< 8 Å[19,20]) of different ^{29}Si framework sites. 2D intensity correlations are observed between the five distinct ^{29}Si signals associated with the nanolayered silicate framework (blue

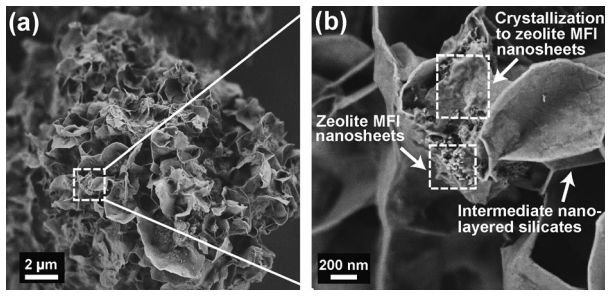

Figure 3. a) Representative SEM image of the intermediate product of crystallizing zeolite MFI nanosheets after 8.5 days of hydrothermal synthesis. b) Enlarged region showing morphologies associated with the intermediate nanolayered silicates, the zeolite MFI nanosheets, and the transformation between them.

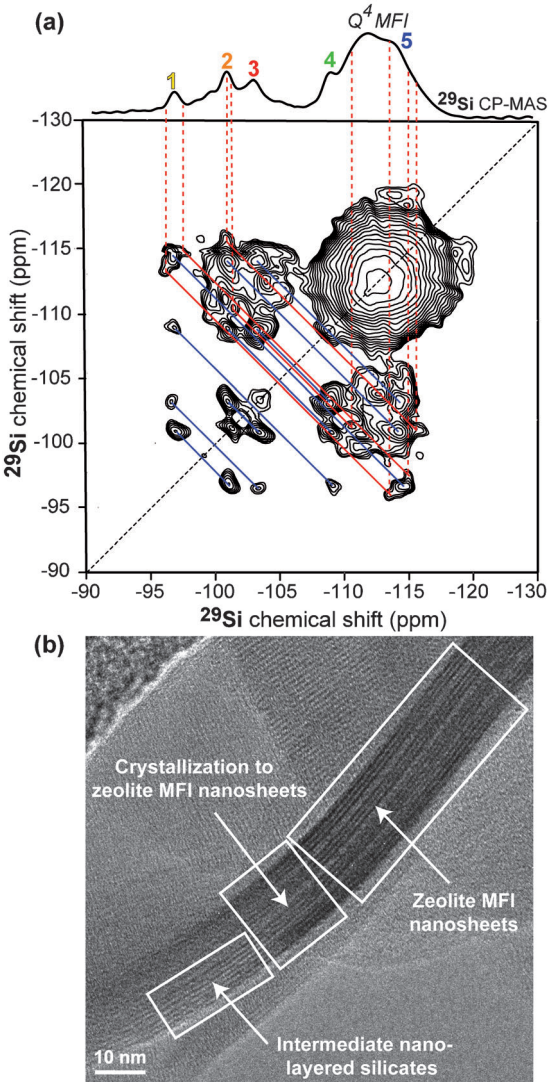

Figure 4. a) Solid-state 2D dipolar-mediated $^{29}Si\{^{29}Si\}$ correlation NMR spectrum of the intermediate product of crystallizing zeolite MFI nanosheets after 10 days of hydrothermal synthesis. A 1D ^{29}Si CP-MAS NMR spectrum is shown along the horizontal axis. b) TEM image depicting a region in which intermediate nanolayered silicates are transforming into zeolite MFI nanosheets.

anti-diagonal lines), establishing sub-nanometer-scale proximities between the different sites that are identical to those previously reported for a 2D silicate framework.[15,16] The broad 2D correlated intensity straddling the spectrum diagonal at approximately −112 ppm is associated with ^{29}Si site pairs among the 24 crystallographically distinct Q^4 sites of the MFI frameworks. This ^{29}Si intensity is also correlated with the broad ^{29}Si signal at approximately −104 ppm from surface Q^3 moieties of the 2.7 nm-thick zeolite nanosheets.

Crucially, 2D intensity correlations are observed (Figure 4a, red anti-diagonal lines) between ^{29}Si signals associated with the transforming nanolayered silicates and the developing crystalline Q^4 ^{29}Si MFI sites, manifesting their sub-nanometer-scale proximities. For example, ^{29}Si signals at approximately −97 and −104 ppm associated with Q^3 sites *1* and *2* in the nanolayered silicates, respectively, are correlated with different ^{29}Si signals from −111 to −116 ppm associated with crystallizing or fully crystalline Q^4 MFI framework sites. These results establish that the nanolayered silicates locally transform into zeolite MFI nanosheets within the same domains, as opposed to dissolving and re-crystallizing into zeolitic structures in different regions. Such observations are corroborated by TEM measurements (Figure 4b) that reveal regions where the nanolayered silicates are crystallizing into zeolite MFI nanosheets, consistent with the TEM and SEM images above.

The different atomic and mesoscopic structures that develop and evolve during hydrothermal crystallization of the zeolite MFI nanosheets are depicted schematically in Figure 5. Initially, the cationic organic surfactants and hydrolyzed anionic silica precursors co-assemble rapidly (ca. seconds to minutes)[21] into MCM-41-like hexagonal mesostructures with amorphous silica frameworks (Figure 5a). Over longer times (ca. days), the di-quaternary ammonium surfactants direct the formation of nanolayered silicates with 2D-crystal-like frameworks (Figure 5b). As the atomically ordered frameworks form, a hexagonal-to-lamellar mesophase transition occurs, reflecting the dominant interactions associated with the crystallizing silicate networks (for which 2D structures are common, e.g., clays), over the much weaker van der Waals interactions associated with liquid-crystal-type structures. Such coupled structural changes are consistent with the large differences in enthalpies associated with zeolite crystallization (ca. −900 kJ mol^{-1}),[22] compared to transitions between self-assembled surfactant phases (ca. −5 kJ mol^{-1} per methyl group[23]). Over longer hydrothermal synthesis times (ca. weeks), the intermediate nanolayered silicates transform into crystalline zeolite MFI nanosheets (Figure 5c), condensing together to an extent that depends on the number of surfactant headgroups and the length of the hydrophobic alkyl linkers. Under hydrothermal synthesis conditions, it is likely that thermal fluctuations allow the pliable nanolayered silicate sheets to make contact and cross-link, as required for their further crystallization (see SI for more details).

Other researchers have reported that zeolites with 3D crystalline frameworks can be synthesized from 2D layered (alumino)silicates, although with important distinctions compared to the results reported here. For example, layered materials have been used as precursors to form MWW-type[24] zeolites (e.g., ITQ-1[25]), ferrierite,[26] as well as new zeolites (e.g., CDS-1[27] and RUB-41[28]). However, such examples have been shown[27,28] or are suggested[26] to involve the topotactic condensation of layered (alumino)silicates during calcination, which retain their local structures as they condense into zeolites. Intermediate layered aluminosilicates have also been reported to form during hydrothermal syntheses of zeolites ZMS-48 and Beta.[29] However, long-range ordering of the intermediate layered frameworks disappeared prior to zeolite formation, suggesting that the layered compounds dissolved and did not transform directly into zeolitic structures.[29] Here, the nanolayered silicates transform into zeolite MFI nanosheets non-topotactically, yet with both framework structures co-existing in sub-nanometer-scale proximities. Collectively, the results indicate that 2D layered (alumino)silicates can transform into 3D zeolitic structures under different pathways and synthesis conditions.

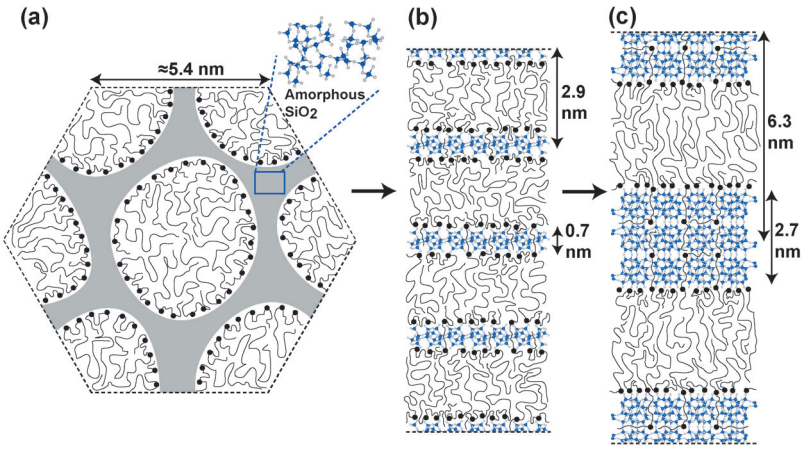

Figure 5. Schematic diagrams of the atomic and mesoscopic material structures that evolve during the hydrothermal crystallization of the zeolite MFI nanosheets: a) initially amorphous silica frameworks (gray) with weak hexagonal mesophase ordering, b) intermediate nanolayered silicates, and c) zeolite MFI nanosheets. Si and O framework atoms are represented by blue and white spheres, respectively. The surfactant headgroups and alkyl chains are represented by black circles and gray lines, respectively.

In summary, the complicated atomic and mesoscale framework transformations that occur during hydrothermal syntheses of mesostructured zeolites are shown to be highly correlated. Here, surfactant-directed mesostructured silica, initially formed with an amorphous framework, transformed slowly into an intermediate nanolayered silicate that subsequently crystallized into self-supporting nanosheets of silicalite-1 with a MFI structure and bimodal sub-nano- and meso-scale porosity. The combined NMR, XRD, and TEM analyses establish the coupled processes and molecular-level interactions that transiently govern framework crystallization and surfactant self-assembly and thereby influence the development and evolution of framework structural order over different length and time scales. The resulting insights

are expected to aid the development of design strategies aimed at synthesizing new surfactant-directed zeolites with different framework structures and mesophase ordering with desirable transport and catalytic properties.

Experimental Section

Materials: Siliceous zeolite MFI nanosheets and intermediate products were synthesized according to the procedure of Na, et al.[3] from the same starting mixture and under identical hydrothermal conditions, except for their reaction times. Detailed synthesis and characterization procedures are described in the SI.

Solid-state NMR spectroscopy: All solid-state NMR experiments were performed under ambient conditions on a Bruker AVANCE IPSO 500 NMR spectrometer with an 11.74 Tesla widebore superconducting magnet operating at 500.13 and 99.35 MHz for ^{1}H and ^{29}Si nuclei. All spectra were acquired at 4.6 kHz (2D $^{29}Si\{^{29}Si\}$ NMR spectrum) or 12.5 kHz (all other NMR spectra) MAS. Additional details are described in the Supporting Information.

Received: August 27, 2014
Published online: November 24, 2014

Keywords: crystallization · layered silicates · mesostructured zeolites · self-assembly · solid-state NMR spectroscopy

[1] M. Choi, K. Na, J. Kim, Y. Sakamoto, O. Terasaki, R. Ryoo, *Nature* **2009**, *461*, 246 – 249.
[2] K. Na, C. Jo, J. Kim, K. Cho, J. Jung, Y. Seo, R. J. Messinger, B. F. Chmelka, R. Ryoo, *Science* **2011**, *333*, 328 – 332.
[3] K. Na, M. Choi, W. Park, Y. Sakamoto, O. Terasaki, R. Ryoo, *J. Am. Chem. Soc.* **2010**, *132*, 4169 – 4177.
[4] W. Park, D. Yu, K. Na, K. E. Jelfs, B. Slater, Y. Sakamoto, R. Ryoo, *Chem. Mater.* **2011**, *23*, 5131 – 5137.
[5] Y. Seo, K. Cho, Y. Jung, R. Ryoo, *ACS Catal.* **2013**, *3*, 713 – 720.
[6] D. P. Serrano, J. Aguado, G. Morales, J. M. Rodríguez, A. Peral, M. Thommes, J. D. Epping, B. F. Chmelka, *Chem. Mater.* **2009**, *21*, 641 – 654.
[7] M. Choi, H. S. Cho, R. Srivastava, C. Venkatesan, D.-H. Choi, R. Ryoo, *Nat. Mater.* **2006**, *5*, 718 – 723.
[8] H. Wang, T. J. Pinnavaia, *Angew. Chem. Int. Ed.* **2006**, *45*, 7603 – 7606; *Angew. Chem.* **2006**, *118*, 7765 – 7768.
[9] C. T. Kresge, M. E. Leonowicz, W. J. Roth, J. C. Vartuli, J. S. Beck, *Nature* **1992**, *359*, 710 – 712.
[10] D. Zhao, J. Feng, Q. Huo, N. Melosh, G. H. Fredrickson, B. F. Chmelka, G. D. Stucky, *Science* **1998**, *279*, 548 – 552.
[11] A. Karlsson, M. Stocker, R. Schmidt, *Microporous Mesoporous Mater.* **1999**, *27*, 181 – 192.
[12] J. S. Beck, J. C. Vartuli, G. J. Kennedy, C. T. Kresge, W. J. Roth, S. E. Schramm, *Chem. Mater.* **1994**, *6*, 1816 – 1821.
[13] S. C. Christiansen, D. Zhao, M. T. Janicke, C. C. Landry, G. D. Stucky, B. F. Chmelka, *J. Am. Chem. Soc.* **2001**, *123*, 4519 – 4529.
[14] Pre-treatment of the TEM samples with acetone resulted in removal of excess surfactant species that led to smaller interlayer spacings in the TEM images, compared to the XRD *d*-spacings measured for the as-synthesized materials (see the Supporting Information for more details).
[15] N. Hedin, R. Graf, S. C. Christiansen, C. Gervais, R. C. Hayward, J. Eckert, B. F. Chmelka, *J. Am. Chem. Soc.* **2004**, *126*, 9425 – 9432.
[16] D. H. Brouwer, S. Cadars, J. Eckert, Z. Liu, O. Terasaki, B. F. Chmelka, *J. Am. Chem. Soc.* **2013**, *135*, 5641 – 5655.
[17] S. Cadars, N. Mifsud, A. Lesage, J. D. Epping, N. Hedin, B. F. Chmelka, L. Emsley, *J. Phys. Chem. C* **2008**, *112*, 9145 – 9154.
[18] C. A. Fyfe, H. Grondey, Y. Feng, G. T. Kokotailo, *J. Am. Chem. Soc.* **1990**, *112*, 8812 – 8820.
[19] D. H. Brouwer, P. E. Kristiansen, C. A. Fyfe, M. H. Levitt, *J. Am. Chem. Soc.* **2005**, *127*, 542 – 543.
[20] D. H. Brouwer, R. J. Darton, R. E. Morris, M. H. Levitt, *J. Am. Chem. Soc.* **2005**, *127*, 10365 – 10370.
[21] A. Firouzi, D. Kumar, L. M. Bull, T. Besier, P. Sieger, Q. Huo, S. A. Walker, J. A. Zasadzinski, C. Glinka, J. Nicol, et al., *Science* **1995**, *267*, 1138 – 1143.
[22] I. Petrovic, A. Navrotsky, M. E. Davis, S. I. Zones, *Chem. Mater.* **1993**, *5*, 1805 – 1813.
[23] A. A. Levchenko, C. K. Yee, A. N. Parikh, A. Navrotsky, *Chem. Mater.* **2005**, *17*, 5428 – 5438.
[24] M. E. Leonowicz, J. A. Lawton, S. L. Lawton, M. K. Rubin, *Science* **1994**, *264*, 1910 – 1913.
[25] M. A. Camblor, C. Corell, A. Corma, M. J. Díaz-Cabañas, S. Nicolopoulos, J. M. González-Calbet, M. Vallet-Regí, *Chem. Mater.* **1996**, *8*, 2415 – 2417.
[26] L. Schreyeck, P. Caullet, J. C. Mougenel, J. L. Guth, B. Marler, *Microporous Mater.* **1996**, *6*, 259 – 271.
[27] T. Ikeda, Y. Akiyama, Y. Oumi, A. Kawai, F. Mizukami, *Angew. Chem. Int. Ed.* **2004**, *43*, 4892 – 4896; *Angew. Chem.* **2004**, *116*, 5000 – 5004.
[28] Y. Wang, H. Gies, B. Marler, U. Müller, *Chem. Mater.* **2005**, *17*, 43 – 49.
[29] A. Tuel, *Chem. Mater.* **1999**, *11*, 1865 – 1875.

